



## Fracture and solid particle erosion of micro-crystalline, nano-crystalline and boron-doped diamond films



Xinchang Wang, Jianguo Zhang, Bin Shen, Tao Zhang, Fanghong Sun \*

School of Mechanical Engineering, Shanghai Jiao Tong University, Shanghai 200240, China

### ARTICLE INFO

#### Article history:

Received 6 November 2013

Accepted 22 February 2014

Available online 28 February 2014

#### Keywords:

CVD diamond film

Fracture strength

Adhesion

Solid particle erosion

Velocity exponent

### ABSTRACT

Chemical vapor deposition (CVD) diamond film has been considered as a good candidate protective coating under hostile and abrasive conditions due to its outstanding erosion behavior. In the present study, the conventional micro-crystalline diamond (MCD) film, nano-crystalline diamond (NCD) film and the boron-doped diamond (BDD) film are respectively fabricated by the hot filament CVD (HFCVD) method. Solid particle erosion tests are conducted on diamond films in an air–sand erosion rig under different impact velocities ( $v$ ) and angles ( $\alpha$ ) with angular SiC sands as the erodents, and WC–Co and SiC materials are adopted as comparisons. The field emission scanning electron microscopy (FESEM), X-ray diffraction (XRD), Raman spectroscopy, Rockwell hardness tester and surface profilometer are respectively used to characterize diamond films before and after tests, exhibiting that compared with MCD and NCD films, the BDD film performs relatively higher fracture strength and better adhesion. Typical solid impact erosion stages of the different diamond films are observed. The solid particle erosion behavior of diamond films has close relationships to their fracture strength and adhesion. As a result, when the impact angle  $\alpha \leq 30^\circ$ , the steady-state erosion rate of the BDD film is lower than those of MCD and NCD ones. More importantly, under all the impact angles and velocities, much quicker film delamination and removal can be noticed on the MCD and NCD films, especially the NCD one. By contrast with WC–Co and SiC materials, diamond films present much better erosion resistance and higher velocity exponents, which should be attributed to different impact mechanisms caused by the different hardness of eroded samples.

© 2014 Elsevier Ltd. All rights reserved.

### Introduction

For many fluid machineries used in mechanical and petrochemical industries, by means of erosion and corrosion processes, solid particles entrained in the gas or fluid flow can cause remarkable degradation of component surfaces suffering impact. Due to the outstanding hardness and erosion–corrosion resistance that approach the single crystal natural diamond, HFCVD diamond films are considered as good candidate protective coatings on components operating under hostile and abrasive conditions, such as the aerospace component suffering severe particle impact, the valve and the nozzle for the multiphase flow [1–4].

Boron doping is a common doping technology in HFCVD diamond film growth, which is proved to be very useful for modifying their electrochemical and tribological behaviors and widely used in the electrochemical and semiconductor industries [5,6]. It's also supposed that boron doping can improve the adhesion between diamond films and

substrates, and some other mechanical and tribological properties [7–9]. Many available researches have been reported to study the solid impact erosion behavior of conventional micro-crystalline diamond (MCD) and nano-crystalline diamond (NCD) films [10–20]. In the previous studies, from the perspective of grain size, it's supposed that compared with the MCD film, the NCD film may be responsible for higher erosion resistance since higher strength is expected in smaller grain size of diamond film [14,16]. In our application research, it has been observed that boron doping technology has positive effects on the solid impact erosion behavior of boron-doped composite diamond films deposited on working surfaces of nozzles owing to the improvement of the adhesion [4]. Moreover, it's imperative to further study the differences between solid impact erosion progresses and mechanisms of boron-doped diamond (BDD), MCD and NCD films from the aspect of not only the grain size and adhesion but also the fracture strength that is much related to the solid impact erosion behavior.

MCD, NCD and BDD films are respectively fabricated by the HFCVD method. Solid particle erosion tests are conducted with an air–sand erosion rig. Focusing on clarifying the solid particle erosion progresses and mechanisms of all the diamond films, the FESEM, XRD, Raman spectroscopy, Rockwell hardness tester and surface profilometer are adopted to characterize diamond films before and after solid particle erosion tests.

\* Corresponding author at: Mechanical Building B344, Dongchuan Road 800, Minhang District, Shanghai 200240, China. Tel.: +86 13641872415.

E-mail addresses: [wangxinchang@sjtu.edu.cn](mailto:wangxinchang@sjtu.edu.cn) (X. Wang), [fnzjg@163.com](mailto:fnzjg@163.com) (J. Zhang), [binshen@sjtu.edu.cn](mailto:binshen@sjtu.edu.cn) (B. Shen), [muogui\\_1016@163.com](mailto:muogui_1016@163.com) (T. Zhang), [sunfanghong@sjtu.edu.cn](mailto:sunfanghong@sjtu.edu.cn) (F. Sun).

## Experimental details

### Deposition and characterization

In this article, SiC ceramics are chosen as substrates due to the relatively better adhesion between diamond films and SiC materials [21]. Three types of diamond films are deposited on SiC plane substrates by the HFCVD method: (I) MCD film; (II) NCD film; and (III) BDD film. Deposited surfaces of substrates are all ground and then polished with the ~15  $\mu\text{m}$  diamond paste to further improve the adhesion between diamond films and substrates. Afterwards, the polished surfaces are diamond seeded by scratching with the diamond powders (0.5–1  $\mu\text{m}$ ), with the purpose of enhancing the nucleation density [22]. A mixture of acetone and hydrogen is used as the common reactant gas, and excessive argon is added in the deposition process of the NCD film. Deposition parameters are all listed in Table 1. During the deposition process of the BDD film, the trimethylborane ( $\text{B}(\text{CH}_3\text{O})_3$ ) is adopted as the boron dopant [23]. The detailed preparation methods of the diamond films can refer to our previous studies [9,24].

The FESEM (Zeiss ULTRA55), XRD (D8 ADVANCE) and Raman spectroscopy (SPEC14-03) are firstly adopted to characterize three types of diamond films before solid particle erosion tests. The Hoytom Rockwell hardness tester with a diamond indenter (angle =  $120^\circ$ , radius = 0.2 mm) is applied to measure their Rockwell hardness (HRA) under a 600 N load. Besides, indentation morphologies on the diamond films under a 1000 N load are also obtained and accordingly ranks of their adhesion and fracture strength are estimated. Every hardness or fracture strength value is averaged over three values obtained from three different static indentation tests conducted under the identical condition in order to minimize the error.

### Solid particle erosion tests

Solid particle erosion tests are conducted in a standard air–sand erosion rig, as illustrated in Fig. 1, adopting the three types of diamond films, WC–Co and SiC plane samples as eroded samples. In the rig, the compressed air is fed through a constricted region. The reduction in cross-sectional area instigates an increase in air speed, which is accompanied by a reduction in pressure, a process known as the Venturi effect, by virtue of which the solid particles are drawn into the airflow and travel down the nozzle. Upon leaving the nozzle, the particles are carried by the air until they impact the sample [25]. Angular SiC sands of 320 mesh (~45  $\mu\text{m}$ ) are chosen as the erodents to obtain their erosion rates under different impact velocities  $v$  (60–140 m/s) and angles  $\alpha$  ( $15^\circ$ – $90^\circ$ ). The impact velocity  $v$  is measured by the double disk method [26]. The erodent flux is fixed as 0.55 g/s and the stand-off distance, from the end of the nozzle to the surface of the sample, is fixed as  $20 \text{ mm} \pm 1 \text{ mm}$ . The aperture of the nozzle is  $\Phi 1.2 \text{ mm}$  and the scattering angle is about  $12^\circ$ , accordingly the extension of the particle flow (the eroded area) can be calculated as  $\Phi 9.7 \text{ mm}$ , which covers 74% of the sample surface ( $10 \text{ mm} \times 10 \text{ mm}$ ). In the scattering region (the eroded area), as-measured particle flow density presents a certain dispersion,

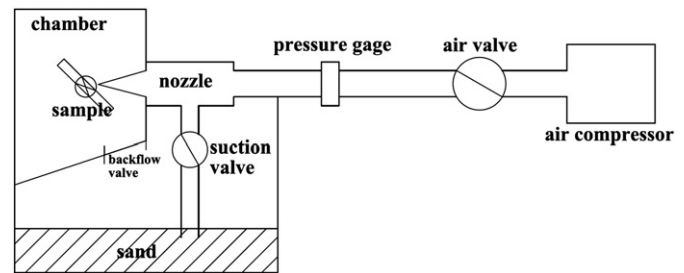


Fig. 1. Schematic diagram of the standard air–sand erosion rig.

so the actual impact angle for a given nominal angle  $\alpha$  should be  $\alpha \pm 12^\circ$ .

Erosion rates for various brittle materials are calculated from mass loss resulting from the erodent impact, which is measured by a precision balance with  $\pm 0.01 \text{ mg}$  accuracy. Before each measurement, ultrasonic is used to clean up erodent fragments on eroded surfaces. In each case, the erosion rate will tend towards a steady state, which is used as one of the criteria of the erosion resistance. Moreover, the failure mechanism of diamond films is also used as another criterion of the erosion resistance. The FESEM, surface profilometer and Raman spectroscopy are adopted to characterize eroded samples in order to clarify their solid particle erosion progresses and further study their erosion mechanisms.

## Results and discussion

### Characterization

Surface and cross-sectional morphologies of as-fabricated diamond films are all shown in Fig. 2. The MCD film shows diamond crystallites of well-defined shapes without steps or any irregularities. The BDD film presents many obvious pentagon defects (as shown in the red circles), and the grain size is a little smaller than that of the MCD film but still in the scale of micron meter. However, the NCD film has very small diamond grains ~50–100 nm in diameter. The film thickness has many effects on the solid particle erosion behavior of the diamond film. As a result, the deposition time for the three types of diamond films is controlled so as to obtain MCD, NCD and BDD films with similar thickness, also as demonstrated in Fig. 2.

Differences of diamond crystal orientations might also have some effects on solid particle erosion behaviors of diamond films at the crystal level, so XRD is adopted to observe diamond crystal orientations of as-fabricated diamond films. According to XRD spectra all the diamond films are mainly  $\langle 111 \rangle$  oriented, as demonstrated in Fig. 3. Therefore the crystal orientation can be neglected in discussions on differences between solid impact erosion mechanisms of the three types of diamond films.

The chemical quality of as-deposited diamond films is evaluated by Raman spectroscopy using a He–Ne laser with an excitation wavelength of 632.8 nm. Raman spectra of all the diamond films are shown in Fig. 4. A pronounced peak located at  $\sim 1338.09 \text{ cm}^{-1}$  with FWHM of  $\sim 7.89 \text{ cm}^{-1}$  is obtained in the Raman spectrum of the MCD film, confirming its high diamond purity and quality. Compared with the natural diamond,  $\text{sp}^3$  peak slightly shifts relative to the stress-free frequency ( $1332 \text{ cm}^{-1}$ ) due to the internal compressive residual stress. In the Raman spectrum of the NCD film, the  $\text{sp}^3$  peak around  $1341.15 \text{ cm}^{-1}$  is significantly broad, which indicates the existence of micro or nano-sized diamond grains but relatively low diamond purity as compared with the MCD film. Besides, the pronounced Raman scattering intensity in the region of  $1400$ – $1600 \text{ cm}^{-1}$  suggests that the grain size of the film has decreased to nanometer scale. Although the non-diamond peak presents significant intensity in the Raman spectrum of the NCD film,

Table 1  
Deposition parameters for all the diamond films.

Sample	I–MCD	II–NCD	III–BDD
Flux of $\text{H}_2$ [sccm]	1100	1100	1100
Flux of Ar [sccm]	0	2500	0
The ratio of acetone to $\text{H}_2$ [vol.%]	1%–3%	1%–3%	1%–3%
B/C [ppm]	0	0	5000
Pressure [Pa]	3000	1200	3000
Filament temperature [ $^\circ\text{C}$ ]	2200–2300	2200–2300	2200–2300
Substrate temperature [ $^\circ\text{C}$ ]	850–900	850–900	850–900
Bias current [A]	2.5	2.5	2.5
Duration [h]	14	12	14

Download English Version:

<https://daneshyari.com/en/article/1603185>

Download Persian Version:

<https://daneshyari.com/article/1603185>

[Daneshyari.com](https://daneshyari.com)